



Cancer Research

Exosomes Released by Melanoma Cells Prepare Sentinel Lymph Nodes for Tumor Metastasis

Joshua L. Hood, Roman Susana San and Samuel A. Wickline

Cancer Res 2011;71:3792-3801. Published OnlineFirst April 8, 2011.

Updated version Access the most recent version of this article at:
doi:[10.1158/0008-5472.CAN-10-4455](https://doi.org/10.1158/0008-5472.CAN-10-4455)

Cited Articles This article cites by 46 articles, 17 of which you can access for free at:
<http://cancerres.aacrjournals.org/content/71/11/3792.full.html#ref-list-1>

Citing articles This article has been cited by 14 HighWire-hosted articles. Access the articles at:
<http://cancerres.aacrjournals.org/content/71/11/3792.full.html#related-urls>

E-mail alerts [Sign up to receive free email-alerts](#) related to this article or journal.

Reprints and Subscriptions To order reprints of this article or to subscribe to the journal, contact the AACR Publications Department at pubs@aacr.org.

Permissions To request permission to re-use all or part of this article, contact the AACR Publications Department at permissions@aacr.org.

Exosomes Released by Melanoma Cells Prepare Sentinel Lymph Nodes for Tumor Metastasis

Joshua L. Hood, Susana San Roman, and Samuel A. Wickline

Abstract

Exosomes are naturally occurring biological nanovesicles utilized by tumors to communicate signals to local and remote cells and tissues. Melanoma exosomes can incite a proangiogenic signaling program capable of remodeling tissue matrices. In this study, we show exosome-mediated conditioning of lymph nodes and define microanatomic responses that license metastasis of melanoma cells. Homing of melanoma exosomes to sentinel lymph nodes imposes synchronized molecular signals that effect melanoma cell recruitment, extracellular matrix deposition, and vascular proliferation in the lymph nodes. Our findings highlight the pathophysiologic role and mechanisms of an exosome-mediated process of microanatomic niche preparation that facilitates lymphatic metastasis by cancer cells. *Cancer Res*; 71(11); 3792–801. ©2011 AACR.

Introduction

To metastasize, tumor cells must manipulate their microenvironment to optimize conditions for deposition and growth both locally and at a distance. In accordance with the "seed and soil" hypothesis for example cancer stem cells or metastatic cells function as "seeds" and a particular organ microenvironment or niche serves as the "soil" (1–3). Potential sites for remote tumor implantation might thus be prepared well ahead of actual metastasis (4).

For specific cancers such a metastatic melanoma, the process of metastasis involves lymphatic dissemination although the precise role lymph nodes play in supporting this process is not defined (5). In one hypothesis melanoma cells undergo simultaneous hematogenous and lymphatic spread and the presence of tumor cells in sentinel or regional nodes is merely indicative of metastasis. Alternatively, sentinel or regional nodes play an active role in the progression of melanoma metastasis. The observation that regional lymph nodes downstream of melanomas undergo reactive lymphangiogenesis prior to metastasis (6) suggest that melanoma metastasis is facilitated by preparation of a premetastatic niche within lymph nodes. This process is believed to be mediated by tumor secretion of paracrine angiogenic growth factors.

In this report, we show an adjunctive and highly efficient model of premetastatic niche formation in regional lymph

nodes through the local actions of melanoma exosomes. Exosomes are naturally occurring biological nanovesicles (~30–100 nm) that are formed by the inward budding of multivesicular bodies (MVB), as a component of the endocytic pathway (7–11). They are generated constitutively and released into the tumor microenvironment and circulation via fusion of MVBs with the tumor cell plasma membrane. The nanoscale size of exosomes facilitates their penetration and interaction with local tumor cells as well as with cell types that are distant to an advancing tumor cell front. This may result in tumor immune evasion by direct suppression of T cell activation and induction of apoptosis (12), suppression of the antitumor activity of natural killer cells (13) and other mechanisms (14).

Recently, we have shown that melanoma exosomes induce alterations in the angiogenic microenvironment using a 3-dimensional culture assay (15). These results suggest that melanoma exosomes may be instrumental in melanoma cell dissemination. These findings support other studies showing increased endothelial tubulogenesis by D6.1A tetraspanin expressing pancreatic cancer cell exosomes (16) or increased migration, proliferation, sprouting, and upregulation of vascular endothelial growth factor receptor 1 (VEGFR-1) on endothelial cells by tetraspanin 8 expressing rat adenocarcinoma cell exosomes (17). Moreover, DII4 (Delta-like 4), a Notch receptor ligand, can be transferred by tumor exosomes to endothelial cells resulting in increased endothelial tubule branching (18).

Thus, in conjunction with the findings of others, our previous observations suggest the presence of a "melanoma exosomal messenger system" that exhibits multifunctional paracrine bioactivities that might facilitate tumor communication within the local tumor microenvironment and distantly through upregulation of angiogenic processes (15). This *in vivo* investigation explores the hypothesis that melanoma exosomes can condition sentinel lymph nodes to become remote niches conducive to the recruitment and growth of melanoma cells.

Authors' Affiliation: Consortium for Translational Research in Advanced Imaging and Nanomedicine (C-TRAIN), Washington University School of Medicine, St. Louis, Missouri

Corresponding Author: Joshua L. Hood, Washington University in Saint Louis, 4320 Forest Park Avenue, Suite 101, Campus Box 8215, Saint Louis, MO 63108. Phone: 314-454-7659; Fax: 314-454-7490; E-mail: jhood@dom.wustl.edu

doi: 10.1158/0008-5472.CAN-10-4455

©2011 American Association for Cancer Research.

The experimental strategy entails production and isolation of melanoma exosomes *in vitro*, followed by preconditioning of nodes with either tumor exosomes versus bland liposomes as a control, and then tumor cell injection and lymphatic tracking to define the molecular signaling events and microanatomic responses that prepare the metastatic turf.

Materials and Methods

Materials and cell culture

Mouse B16-F10 (CRL 6475) melanoma cells and media were purchased from American Type Culture Collection (August 2008), MAP (mitogen-activated protein), and mycoplasma tested for purity and kept frozen at -80°C under liquid nitrogen until resuscitated for use. For culture, cells were maintained with 90% DMEM (Dulbecco's modified Eagle's medium) and 10% heat inactivated FBS at 37°C and 5% CO_2 . Male 6- to 8-week old albino C57/BL6 mice, B6(Cg)-*Tyr^{c-2/J}*, were purchased from Jackson Laboratories and maintained on a normal diet until use. Animal care was in accordance with institutional guidelines. Albino mice were used to minimize fluorescent absorption by melanin leading to signal loss. Fluorescent lipophilic tracers DiO (3,3'-dihexadecyloxycarbocyanine Ex. 484/Em. 501), DiI (1,1'-dioctadecyl-3,3,3',3'-tetramethylindocarbocyanine Ex. 549/Em. 565), DiD (1,1'-dioctadecyl-3,3,3',3'-tetramethylindocarbocyanine Ex. 644/Em. 665), and DiR (1,1'-dioctadecyl-3,3,3',3'-tetramethylindotricarbocyanine Ex. 750/Em. 780) were purchased from Invitrogen.

Isolation and labeling of exosomes

B16-F10 melanoma exosomes were isolated for use in experiments according to previously established methods (15). Briefly, B16-F10 melanoma cell cultures were grown to 70% confluence in three 300 cm^2 flask. Culture media was removed and cells washed in PBS. Cells were cultured for 48 hours in the presence of conditioned media. Conditioned culture media was prepared by subjecting normal culture media to overnight ultracentrifugation at $110,000 \times g$ to remove bovine exosomes (19). B16 melanoma exosomes were collected from 48-hour culture in conditioned media through standard differential centrifugation steps using a 70 Ti rotor (19). Culture media was spun and supernatants collected from $300 \times g$ for 10 minutes, $2,000 \times g$ for 10 minutes, to remove residual cells and debris, $10,000 \times g$ for 30 minutes to remove microparticles (20) and $100,000 \times g$ for 2 hours in the presence or absence of 1.0 $\mu\text{mol/L}$ DiI or DiR. Exosome pellets were washed 3 times in PBS, pooled, and reisolated in PBS at $100,000 \times g$ for 2 hours. Exosome pellets were resuspended in 1 mL of PBS, protein content measured via BCA absorbance (Thermo Fisher Scientific Inc.) and stored at -80°C until use. Between the $10,000$ and $100,000 \times g$ centrifugation steps, exosomes were sized using dynamic light scattering (DLS) as previously reported (15) and the electrokinetic potential (zeta potential) of purified exosomes in PBS was measured using a Zeta Plus Zeta Potential Analyzer (Brookhaven Instruments Corp.). Previously, fluorescent exosome localization technique (FELT) was used to confirm the use of differential

centrifugation and DLS in obtaining a purified population of B16-F10 melanoma exosomes from conditioned media (15). Using FELT, B16-F10 melanoma exosomes applied to continuous sucrose gradients (2.0–0.25 mol/L sucrose, 20 mmol/L HEPES/NaOH, pH 7.4), were found to have a density of (1.10–1.21 g/mL; ref. 15).

Construction of fluorescent control liposomes

A lipid commixture including 64.89 mol% lecithin (phosphatidylcholine, Avanti Polar Lipids Inc.), 32.08 mol% cholesterol (Sigma-Aldrich Co.), 3.02 mol% phosphatidylethanolamine (Avanti Polar Lipids Inc.), and 0.01 mol% DiD was solubilized in chloroform, and dried to a lipid film under continuous vacuum using a rotary evaporator. Residual solvent was removed by overnight drying under continuous vacuum. The dry lipid film was resuspended in 20 mL of distilled deionized water, and emulsified (Microfluidics Corp.) at 20,000 psi for 4 minutes to form liposomes. Liposomes in PBS were sized using DLS and zeta potential determined using a Zeta Plus Zeta Potential Analyzer (Brookhaven Instruments Corp.).

Nodal trafficking of liposomes, exosomes, or cells

Fluorescent DiR or DiI labeled exosomes (50 μg), DiD-liposomes, or DiO-B16-melanoma cells (1 million) were each injected into the footpads of individual mice using established techniques (21). To equalize the number of liposomes and exosomes injected, a standard curve relating counts of various particle concentrations of liposomes, designed to be approximately the same size (~ 100 nm) as B16-F10 melanoma exosomes was constructed on the basis of DLS (Brookhaven Instruments Corp.). A best fit equation with $R^2 \sim 1.0$ was then generated and used to mathematically predict the number of exosomes present in a 50 μg sample. On the basis of this calculation, an equivalent number of DiD-liposomes in PBS (50 μL) to 50 μg of DiR-exosomes in PBS (50 μL) were used. A similar standard curve was constructed for DiO labeled melanoma cells to convert fluorescent efficiency values as measured using a Xenogen *in vivo* imaging system (IVIS) Spectrum Workstation (Caliper Life Sciences) to cell numbers.

Lymph node dissection and fluorescent microscopy

Animals were anesthetized with 2.5% isoflurane and euthanized by cervical dislocation under deep anesthesia. The left and right popliteal (PO) or inguinal (IN) murine lymph nodes as mapped by Harrell and colleagues (21) were dissected, frozen at -80°C in OCT (optimal cutting temperature) medium, imaged for liposome, melanoma exosome, and melanoma cell fluorescence using a Xenogen *in vivo* imaging system and cryosectioned. Central frozen tissue cross-sections (8 μm thick) were fixed in acetone, stained for nuclei using VECTASHIELD mounting medium with DAPI (Vector Laboratories Inc.) and visualized using fluorescent microscopy to detect fluorescent carbocyanine-labeled exosomes or cells within nodes or stained with eosin-haematoxylin to verify the structure of the lymphoid tissue.

Real time reverse transcriptase (RT-RT) PCR analysis of lymph nodes

Dissected lymph nodes were solubilized using Qiagen Qiazol solution and total RNA isolated using the Qiagen miR-Neasy Mini kit (Qiagen Inc.) according to the handbook protocol. For each node, 1 μ g of total RNA was converted to cDNA using the RT2 first strand kit (C-03, SABiosciences) and analyzed on the SABiosciences PAMM-024 mouse angiogenesis array with an Applied Biosciences 7300 real-time PCR machine. Even though the same amount of cDNA was applied to each array for either liposome or exosome treated nodes, these experimental conditions have not been assessed before and thus we further sought to standardize the amount of biological material between arrays. Using the method described by Mane and colleagues, we determined the best normalization gene (tissue inhibitor of metalloproteinase 2) across 6 initial arrays (3 liposome and 3 exosome nodes) for our experimental conditions based on the criteria of minimal C_t variance, as reflected by lowest SD, and highest normality of distribution (22). Normality of distribution was determined using JMP Version 8 (SAS Institute) statistical software.

Statistics

To determine the statistical significance between the fluorescent distributions of individual lymph nodes, the 2-tailed Student's *t* test was used to calculate *P* values for $\alpha = 0.05$. For comparing overall lymph node [left (L) PO, right (R) PO, L IN, R IN] distribution patterns between liposomes, exosomes, melanoma cells chasing liposomes, and melanoma cells chasing exosomes groups, JMP Version 8 (SAS Institute) statistical software was utilized according to product instructions (<http://www.jmp.com/support/notes/30/584.html>) for replicate data ($n = 5$) using the univariate approach (*F* ratio = 5.94, $P < 0.0001$) so as not to exclude nodes containing a replicate measurement(s) where percentage of fluorescent signal distribution = 0. Thus, a standard least squares matrix table was constructed and least squares means differences student's *t* analysis carried out on all possible pairings between lymph node subtypes (exosome L PO vs. liposome L PO or liposome L PO vs. cells chasing liposomes L PO, etc.) assuming a random normal distribution and $\alpha = 0.05$. For RT-RT PCR array analysis, RT2 Profiler PCR Array Software (SABiosciences) incorporating a 2-tailed Student's *t* test was used to calculate *P* values for $\alpha = 0.05$ (<http://pcrdataanalysis.sabiosciences.com/pcr/arrayanalysis.php>)><http://pcrdataanalysis.sabiosciences.com/pcr/arrayanalysis.php>).

Results

Melanoma exosomes home to sentinel lymph nodes

Given the predilection of melanoma to metastasize via lymphatics, we hypothesized that melanoma exosomes travel to sentinel lymph nodes. To the best of our knowledge this is the first study of its kind to assess lymphatic trafficking of any type of exosome. Therefore, we constructed a control liposome to determine whether trafficking patterns would differ between melanoma exosomes versus inert bland nanovesicles lacking protein, mRNA, miRNA, or other complex molecular

variables found in exosomes (23–25). On the basis of our experience formulating stable nanoparticles, we constructed liposomes containing phosphatidyl choline (64.89 mol%), phosphatidyl ethanolamine (3.02 mol%), cholesterol (32.08 mol%) and a negligible amount of DiI (0.01 mol%) fluorescent label. These lipids are common components of exosomes (26–28). The use of these lipid ratios produced liposomes with a size (98 ± 4 nm) and electrokinetic (zeta) potential (-8 ± 2 mV) that closely approximate that of B16-F10 melanoma exosomes (95 ± 14 nm and -11 ± 5 mV). Thus, DiI labeled B16-F10 melanoma exosomes or an equivalent number of control DiI labeled bland liposomes were injected into the footpads of albino C57/BL6 mice as described (21). Mouse feet are drained by a corresponding right and left pair of PO and IN lymph nodes (21). Thus, these nodes serve as sentinel nodes for footpad tumors. The IN nodes were chosen for extraction and analysis in this experiment rather than the PO nodes because we anticipated the potential for increased cross-trafficking between the more distal left and right IN lymphatics than the local sentinel PO nodes. Moreover, we sought to determine whether melanoma exosomes are capable of traveling long distances from the injection site. These sentinel nodes were obtained 48 hours after injection of liposomes or melanoma exosomes into the right or left footpad, respectively (Fig. 1A). IN nodes were collected for each mouse ipsilateral or contralateral to the footpad injection site of liposomes or exosomes and scanned for fluorescent signals using IVIS (Fig. 1B). The results show a significant homing preference of melanoma exosomes to the IN node ipsilateral to the injection site (Fig. 1C). In contrast, the liposome signal was distributed evenly in IN nodes both ipsilateral and contralateral to the injection site. Additionally, there was no difference in the average size of lymph nodes (Fig. 1D) or number of nucleated cells (Fig. 1E) present in either the ipsilateral or contralateral lymph nodes 48 hours following footpad inoculation with either liposomes or melanoma exosomes. Taken together, these data show a prominent and focal selectivity of melanoma exosome homing to the ipsilateral "sentinel" lymph nodes when compared with liposomes of similar size.

Melanoma exosomes influence the lymph node distribution pattern of free melanoma cells

On the basis of the short-term homing pattern of melanoma exosomes relative to liposomes (Fig. 1), we hypothesized that melanoma exosomes may influence how free melanoma cells distribute within a lymphatic microenvironment during metastasis. To approximate a metastatic process *in vivo*, we serially injected the left footpad of 2 groups of mice 3 times, once every 48 hours, with either liposomes or melanoma exosomes. For the third injection, we included 1 million fluorescent green (carbocyanine, DiO) labeled melanoma cells. Footpad tumors were visually apparent at 10 days in both groups. The average mass of the tumor sections obtained for the liposome and exosome mice groups was similar (33 and 34 mg, respectively).

Ipsilateral and contralateral IN and PO lymph nodes were harvested from both groups of animals to assess the lymphatic distribution pattern of melanoma cells following

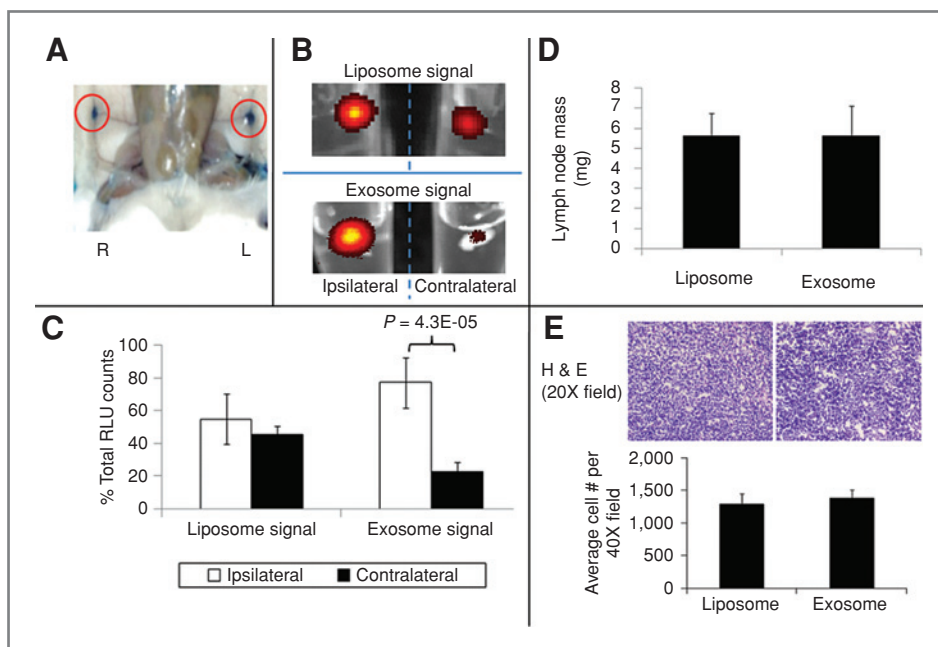


Figure 1. Melanoma exosome versus control liposome IN lymph node distribution *in vivo* at 48 hours. A, albino C57/BL6 mice were anesthetized under 2.5% isoflurane and footpads injected with 2.5% Evans Blue dye in 25 μ L PBS to visualize lymph nodes (21). At 20-minute postinjection, mice were euthanized, dissected, and right (R) and left (L) IN nodes visualized (red circles). B, DiD-liposome versus DiR-exosome signal detected by IVIS in representative pairs of IN nodes ($n = 6$) both ipsilateral and contralateral to the footpad injection site. C, DiD-liposome versus DiR-exosome average signal distribution in IN nodes ($n = 6$ pairs). Error bars represent SEM. D, following dissection, IN lymph nodes were weighed for comparison between liposome and exosome treated nodes ($n = 5$ pairs); error bars represent SD. E, using H&E staining, the number of nucleated cells in DiD-liposome or DiR-exosome treated nodes were counted and averaged for ($n = 15$) random fields obtained from 3 nodes for each treatment with 5 fields per node; error bars represent SD. Statistically significant relationships are delineated by connecting bars. Rounded P values are listed above the connecting bars; P values < 0.05 were considered statistically significant.

prior inoculation with liposomes or exosomes. We chose the L PO and L IN nodes because they are known to drain the left footpad injection site. R PO and R IN nodes were chosen given the potential for bilateral lymphatic cross-trafficking of nanovesicles showed previously (Fig. 1C). Fluorescent signals for melanoma cells, exosomes or liposomes were quantified for each node using IVIS. No difference in the lymphoid mass among any of the nodes was found with the exception of the ipsilateral L PO node, where the exosome treated group resulted in larger nodes (Fig. 2A). To normalize against any differences in particle or cell loading and fluorescence signal emission efficiencies between different dyes, all fluorescence signals for liposomes, exosomes, cells chasing liposomes, and cells chasing exosomes were converted to percent distribution for each mouse and averaged. This revealed a difference between the distribution of exosomes and liposomes in the L PO and R IN nodes (Fig. 2B). Additionally, we converted the fluorescent signal for melanoma cells to an approximate cellular number using a standard curve relating fluorescence efficiency to cell number. This approach revealed no difference in the total cellular signal in the 4 nodes for each mouse between the liposome or exosome inoculated groups (Fig. 2C). We next compared the internodal and intranodal distribution pattern between particle and melanoma cellular groups using least squares

matrix analysis (F ratio = 5.94, $P < 0.0001$). This revealed a significant difference between the melanoma cellular distribution pattern in the L PO nodes of animals pretreated with melanoma exosomes (Fig. 2D) that could be correlated to the difference in distribution patterns observed for liposomes and exosomes (Fig. 2B). These findings were further supported by fluorescent microscopy comparison of L PO nodes showing an increase in the number of melanoma cells infiltrating the larger node for the exosome versus liposome inoculation groups. This increase was preferentially located in the periphery of the node (Fig. 2E).

Melanoma exosomes enhance migration of melanoma cells to melanoma exosome rich sites in sentinel lymph nodes

On the basis of the results of the melanoma cell recruitment experiments, we hypothesized that melanoma exosomes home to melanoma exosome sites in sentinel lymph nodes and were thus responsible for the difference in the pattern of distribution between melanoma cells chasing liposomes compared with melanoma cells chasing exosomes in the L PO node. To further investigate this hypothesis, additional longer term experiments (10 days) were carried out as described in the previous section. Analysis of inter-group comparisons between liposomes and cells chasing liposomes groups revealed no difference [Fig. 3A (i)].

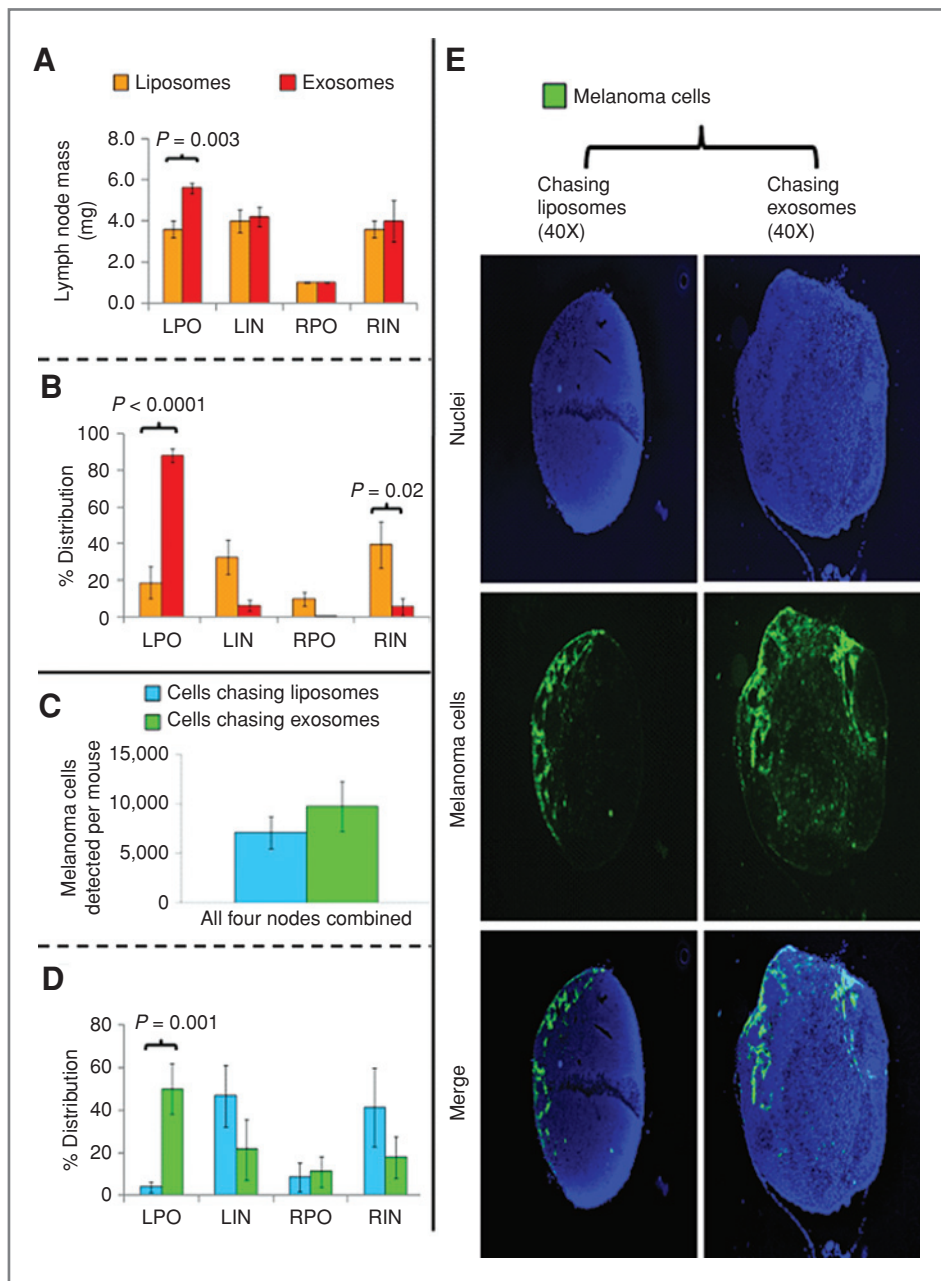


Figure 2. Lymph node distribution of melanoma cells in liposome versus exosome treatment groups post 10 days tumor challenge. **A**, average lymph node mass for 4 liposome versus melanoma exosome treated lymph nodes (L PO, L IN, R PO, R IN). Error bars represent SD ($n = 5$ mice). **B**, distribution pattern of liposomes and melanoma exosomes. Error bars represent SEM ($n = 5$ mice). **C**, average number of melanoma cells detected for all 4 liposome or exosome treated nodes. Error bars represent SD ($n = 5$ mice). **D**, distribution pattern of melanoma cells in liposome or exosome treatment groups. Error bars represent SEM ($n = 5$ mice). **E**, fluorescent microscopy of central L PO lymph node cross-sections in cells chasing liposomes versus exosomes treatment groups; representative of ($n = 5$) mice. Any statistically significant relationships are delineated by connecting bars. Rounded P values are listed above the connecting bars; P values < 0.05 were considered statistically significant. Nuclei of lymph node cells were stained with DAPI (blue). Melanoma cells were fluorescently stained with DiO (green) before injection.

Intragroup comparisons within the liposome group showed a difference in distribution between the R PO and R IN nodes [Fig. 3A (ii)]. The R PO versus R IN difference was also confirmed within the cells chasing liposomes group [Fig. 3A (iii)]. However, in contrast to the liposomes group [Fig. 3A (ii)], the cells chasing liposomes group [Fig. 3A (iii)] also contained differences between the L PO and L IN nodes and the L IN and R PO nodes. Combined, the results of intergroup and intragroup comparisons revealed both similarities and differences between the nodal distribution of liposomes versus cells chasing liposomes groups. For example, more liposomes [Fig. 3A (ii)] than cells chasing lipo-

somes [Fig. 3A (iii)] distributed to the L PO node. In contrast, more cells chasing liposomes [Fig. 3A (iii)] than liposomes [Fig. 3A (ii)] distributed to the L IN node.

Analysis of intergroup comparisons between exosomes and cells chasing exosomes revealed no difference in the distribution pattern with the exception of the L PO node [Fig. 3B (i)]. Fluorescent microscopy analysis confirmed this finding showing more exosome signal in the L PO node cross-section than melanoma cell signal (Fig. 3C). Analysis of intragroup comparisons of the exosomes [Fig. 3B (ii)] and cells chasing exosomes groups [Fig. 3B (iii)] revealed the same differences between the L PO node and the L IN, R PO,

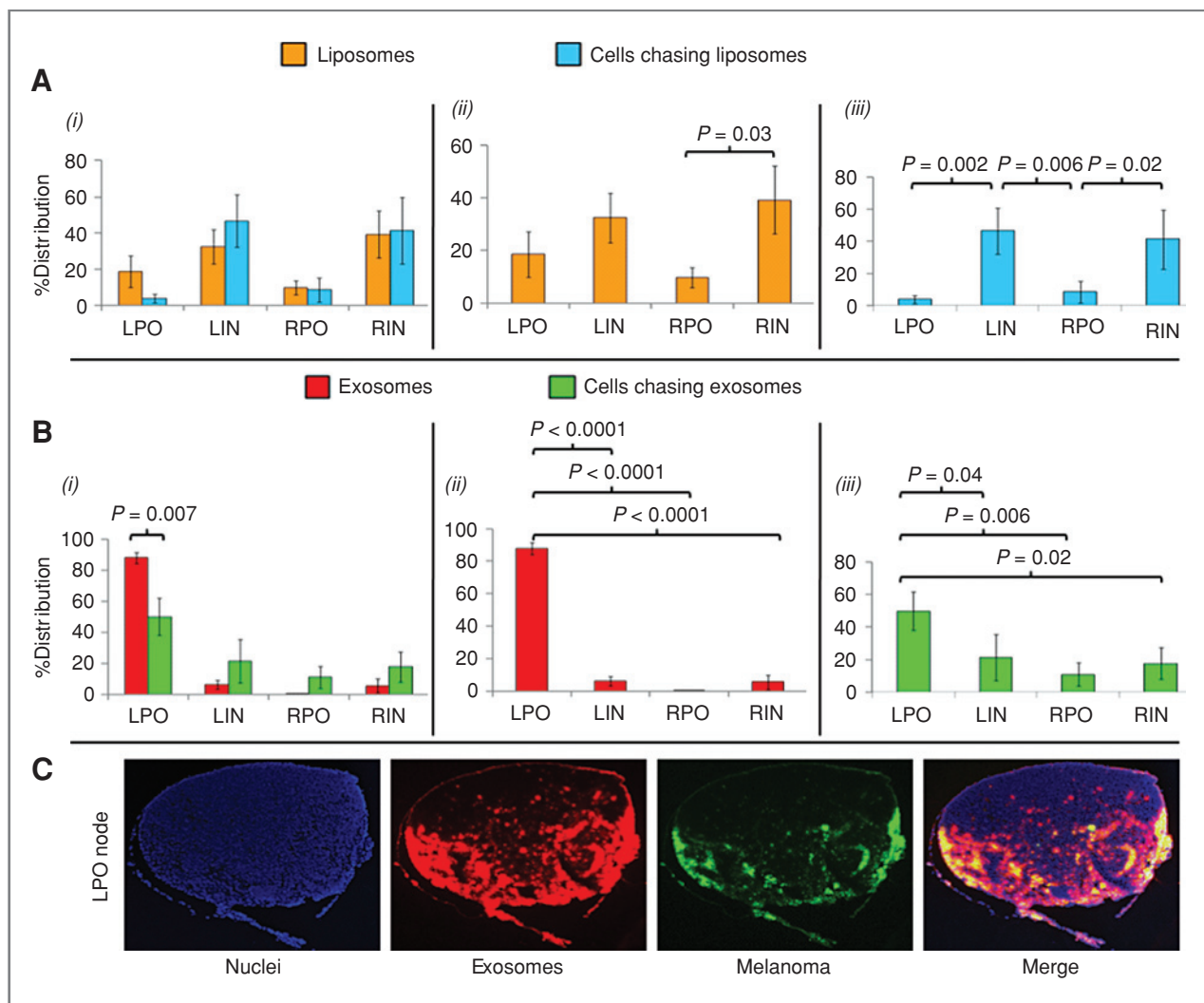


Figure 3. Lymph node distribution of melanoma versus liposome treatment groups post 10 days tumor challenge. A, distribution pattern of liposomes and cells chasing liposomes. Intergroup distribution (i), liposome intragroup distribution (ii), and cells chasing liposomes intragroup distribution (iii). B, distribution pattern of exosomes and melanoma cells chasing exosomes. Intergroup distribution (i), exosome intragroup distribution (ii), and cells chasing exosomes intragroup distribution (iii). C, fluorescent microscopy of a central left PO lymph node cross-section in the exosome treatment group. Error bars represent SEM for ($n = 5$) mice. Any statistically significant relationships are delineated by connecting bars. Rounded P values are listed above the connecting bars; P values < 0.05 were considered statistically significant. Nuclei of lymph node cells were stained with DAPI (blue). Melanoma cells were fluorescently stained with DiO (green) and melanoma exosomes with Dil (red) before injection.

and R IN nodes. Similar to the 48-hour experiment (Fig. 1C), the majority of exosome [Fig. 3B (ii)] versus liposome [Fig. 3A (ii)] signal localizes ipsilateral to the left footpad injection site.

These data show that melanoma cells assume a random lymphatic distribution pattern similar to but not identical to that of inert bland liposomes when chasing liposomes. However, if melanoma cells chase melanoma exosomes, the melanoma cells assume the same pattern of distribution as the exosomes where the majority of signal for both cells and exosomes is found in the significantly larger L PO node [Fig. 3B (i)] closest to the left footpad injection site.

Melanoma exosome dependent lymph node metastasis is driven by induction of multiple metastatic pathways

Taken together, the results of our previous experiments show melanoma exosome dependent recruitment of melanoma cells to exosome rich sites in sentinel lymph nodes. On the basis of these results, we hypothesized that the mechanism of melanoma exosome dependent lymph node metastasis is induction of metastatic pathways conducive to the trapping and growth of melanoma cells. We expected induction in the larger PO sentinel nodes, but opted to determine whether a single dose of melanoma exosomes could travel to and induce metastatic pathways long range in the more distal and less

obvious IN sentinel nodes. We reasoned that this would more accurately show the potency of exosome influences on distal lymph node microenvironments as would be encountered with widespread metastasis. For these experiments, we normalized the gene expression in the R IN node (liposomal) and used it as the baseline for comparison to melanoma exosome induced gene expression in the L IN node. Thus, we compared left and right IN nodes for differential gene expression in mice at 48 hours post a single dose of exosome (left) and liposome (right) footpad injections in individual mice. Of 84 paired genes assessed using an RT-RT PCR array, we discovered 13 significant differences ($P < 0.05$; Fig 4). To simplify interpretation, we subdivided the identified genes into 3 groups: cell recruitment (Fig. 4A), extracellular matrix (Fig. 4B) and vascular growth factors (Fig. 4C). Overall, the array results show that melanoma exosomes enable diverse modes of gene induction within sentinel lymph nodes associated with traditional angiogenic pathways to the establishment of matrix architecture conducive to tumor recruitment and growth.

Discussion

Metastatic progression is a complicated interplay between signaling molecules, tumor cells, and immune cells that will likely differ between different tumor cell types that may or may not produce exosomes. Normal immune and nonimmune exosomes are also likely to be involved in this process. Future experiments will be required to tease apart the complex interchange between normal and tumor exosomes at all stages of metastasis. To the best of our knowledge, our findings are the first to directly show native melanoma exosome induced lymph node conditioning *in vivo*. These findings are limited to exosomes as contrasted to microparticles based on their characteristic features of differential density, size, and morphology (15, 19).

Herein we present a novel tumor exosome dependent model of lymphatic metastatic progression that supports the hypothesis that preconditioned regional or sentinel lymph nodes play an active role in the progression of metastasis (5). We show that melanoma exosomes home to sentinel lymph nodes *in vivo* (Fig. 1). Furthermore, we show that melanoma exosomes can recruit melanoma cells to sentinel lymph nodes (Figs. 2 and 3). Finally, in the absence of melanoma cells, the mechanism of action responsible for this process is melanoma exosome dependent induction of metastatic factors (Fig. 4).

Thus metastatic factors responsible for the recruitment of melanoma cells to sentinel nodes are upregulated by melanoma exosomes themselves. Stabilin 1 (MS-1) expression on vasculature (29) is correlated to melanoma metastasis while upregulation of ephrin receptor $\beta 4$ promotes migration and proliferation of melanoma cells (30, 31). Additionally, melanoma cells derived from lymphatic metastasis express integrin $\alpha_v\beta_3$ which allows their recruitment to lymph nodes through interactions with vitronectin (32).

Our data further show that induction of sentinel nodes by melanoma exosomes increase the expression of a network of interconnected extracellular matrix factors that may promote trapping of melanoma cells within sentinel node niches.

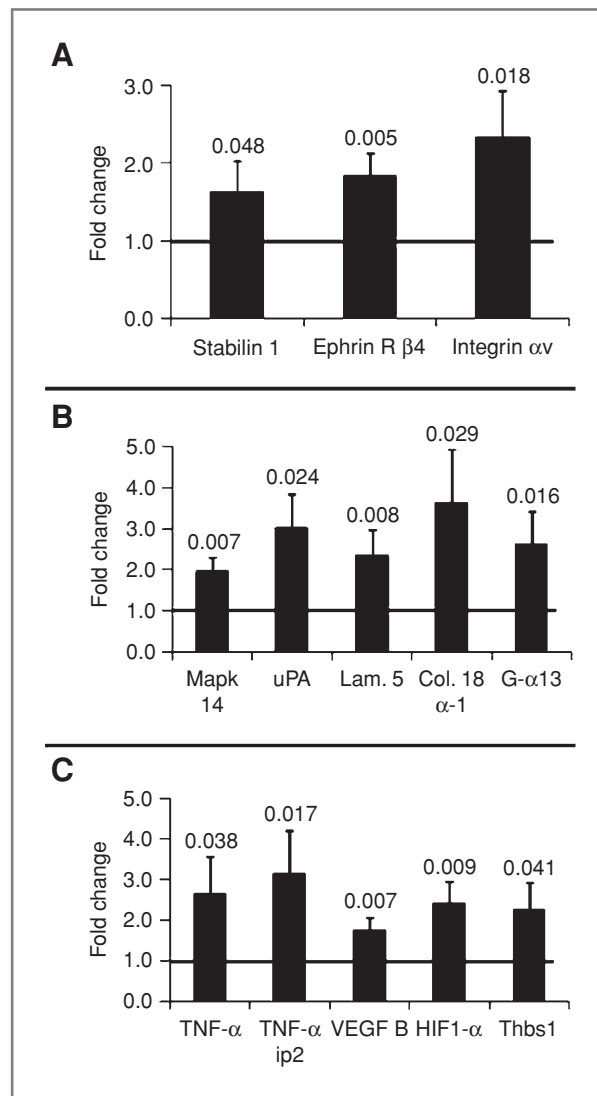


Figure 4. RT-RT PCR analysis of exosome versus control liposome induced gene expression in IN lymph nodes at 48 hours. Bars represent average fold changes for induction of sentinel node factors related to A, melanoma cell recruitment to sentinel nodes; B, matrix modifiers promoting trapping of melanoma cells within sentinel nodes; and C, angiogenic growth factors promoting melanoma growth in sentinel nodes. Control (liposome) fold changes are all normalized to 1 (cross-bar). Error bars represent the SEM for ($n = 6$) arrays. Rounded P values are listed above the error bars for each gene; P values < 0.05 were considered statistically significant. R, receptor; Mapk, map kinase; Col., collagen; Lam., laminin; ip2, inducible protein 2.

MAPK 14 (p38; ref. 33), urokinase plasminogen activator (uPA) protease (34), collagen 18 (35), and laminin 5 (36) derivatives can remodel node stroma to permit basement membrane invasion by tumor cells, while G- α 13 signaling is required for vascular organization during these processes (37).

Finally, the presence of melanoma exosomes in lymph nodes leads to induction of angiogenic growth factors necessary for melanoma growth. VEGF-B expression is increased by metastatic melanoma cells (38) and maintains survival of

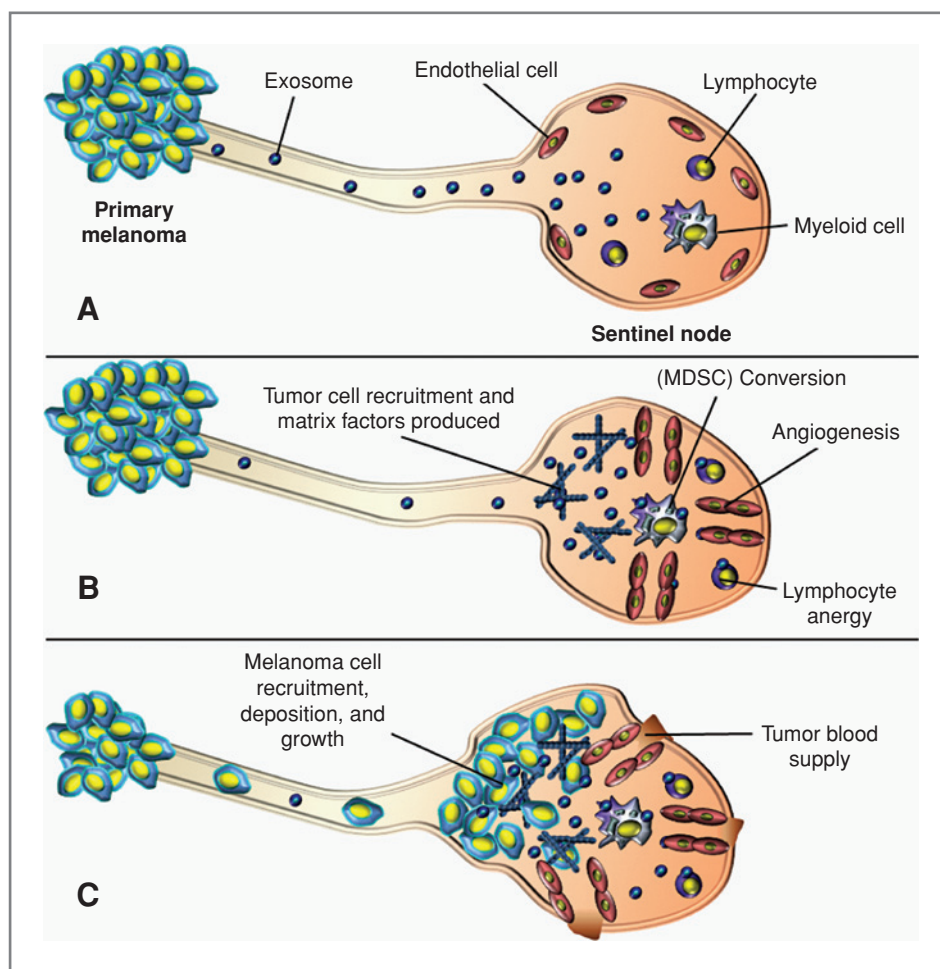


Figure 5. Preparation of sentinel lymph nodes for tumor metastasis by melanoma exosomes. A, melanoma exosomes home to sentinel lymph nodes. B, within sentinel nodes, melanoma exosomes prepare a premetastatic niche by inducing expression of factors responsible for cell recruitment, matrix remodeling, and angiogenesis (15) and likely mediate immunosuppression (12, 45). C, metastatic melanoma or stem cells travel to the prepared niche where they encounter a microenvironment conducive to tumor cell adherence and growth.

neovasculature (39). Increased hypoxia inducible factor 1 α (HIF1- α) expression by melanoma cells contributes to malignancy (40), increased VEGF expression (41), and poor prognosis (42). Paradoxically, thrombospondin 1 (Thbs1) can act on normal peripheral vasculature to increase melanoma blood flow at the expense of peripheral flow (43) and may therefore promote increased sentinel node blood flow conducive for tumor growth.

Tumor microenvironment associated tumor necrosis factor α (TNF- α) promotes melanoma growth and angiogenesis (44). Furthermore, TNF- α is upregulated by myeloid derived suppressor cells (MDSC) induced by melanoma microvesicles and granulocyte-macrophage colony stimulating factor (GM-CSF; ref. 45). Induction of TNF- α therefore signifies simultaneous upregulation of angiogenic and immunosuppressive activities by native melanoma exosomes in the lymph node microenvironment. This supports our previous work showing simultaneous induction of angiogenesis and immunosuppressive factors (GM-CSF and TNF- α) by melanoma exosomes (15) and is consistent with other *in vitro* reports showing melanoma microvesicle mediated "counterattack" of antitumor T-cells (8) and induction of MDSCs (11, 46) which suppress antitumor T-cell function (45).

Collectively, increased gene expression of cell recruitment, extracellular matrix, and vascular proliferation factors by melanoma exosomes produces a niche within sentinel node microenvironments conducive to melanoma cell recruitment, trapping and growth. Essentially, melanoma exosomes serve as the "seed" and sentinel nodes the "soil" for melanoma metastasis. This "turf preparation" response is further supported by our data showing that the pattern of tumor cell recruitment is not random, in contrast to that observed for cells chasing inert liposomes. Rather, trafficking after exosomes is preferential for localization to sentinel nodes closest to footpad tumors. This is exemplified by the recruitment of the majority of melanoma cells to the left PO sentinel node where they are buffered by an even greater number of melanoma exosomes. Given our data and the numerous reports of tumor exosome-mediated immune suppression (11–13), it seems logical that tumor exosomes would have a role in conditioning sentinel lymph nodes for the controlled spread of metastasis whereby routes of communication between primary and metastatic tumors can be efficiently maintained.

The complexity of the mechanism of action of melanoma exosomes on sentinel nodes implies additional testable

hypotheses. Chief among them is whether the component parts of melanoma exosomes coordinately or independently signal nodal preparation: i.e., what is the role of surface molecular epitopes derived from the melanoma parent cell versus their contained cargos. Essentially, exosomes carry and protect fragile mRNA, miRNA, and proteins within their core (23–25). Without this protective environment and molecular targeting by a lipid shell, free mRNA or miRNA would otherwise be rapidly degraded (47) and exosome contents rendered undeliverable and ineffective. Furthermore, the exosome shell necessarily expresses a specific configuration of targeting motifs required for their interaction and communication with target cells.

In our previous report, melanoma exosomes were observed to influence endothelial tubule morphology and stimulate the production of endothelial spheroids and sprouts in a dose-dependent manner (15). In concert, tumor exosomes simultaneously elicited paracrine endothelial signaling by regulation of certain inflammatory cytokines. Taken together, these findings show that melanoma exosomes are capable of directly tuning a remote lymph node toward a microenvironment that facilitates melanoma growth and metastasis in lymph nodes even in the local absence of tumor cells (Fig. 5). Thus melanomas and perhaps other tumors can take advantage of an efficient exosomal messenger mechanism to signal site preparation for eventual metastasis that is accomplished through premetastatic conditioning of lymph nodes by a vanguard of tumor exosomes.

References

- Kaplan RN, Rafii S, Lyden D. Preparing the "soil": the premetastatic niche. *Cancer Res* 2006;66:11089–93.
- Psaila B, Lyden D. The metastatic niche: adapting the foreign soil. *Nat Rev Cancer* 2009;9:285–93.
- Talmadge JE, Fidler IJ. AACR centennial series: the biology of cancer metastasis: historical perspective. *Cancer Res* 2010;70:5649–69.
- Bidard F-C, Pierga J-Y, Vincent-Salomon A, Poupon M-F. A "class action" against the microenvironment: do cancer cells cooperate in metastasis? *Cancer Metastasis Rev* 2008;27:5–10.
- van Akkooi AC, Verhoef C, Eggermont AM. Importance of tumor load in the sentinel node in melanoma: clinical dilemmas. *Nat Rev Clin Oncol* 2010;7:446–54.
- Rinderknecht M, Detmar M. Tumor lymphangiogenesis and melanoma metastasis. *J Cell Physiol* 2008;216:347–54.
- Schorey JS, Bhatnagar S. Exosome function: from tumor immunology to pathogen biology. *Traffic* 2008;9:871–81.
- Martinez-Lorenzo MJ, Anel A, Alava MA, Pineiro A, Naval J, Lasierra P, et al. The human melanoma cell line MeJuSo secretes bioactive FasL and APO2L/TRAIL on the surface of microvesicles. Possible contribution to tumor counterattack. *Exp Cell Res* 2004;295:315–29.
- Admyre C, Johansson SM, Paulie S, Gabrielson S. Direct exosome stimulation of peripheral human T cells detected by ELISPOT. *Eur J Immunol* 2006;36:1772–81.
- Lakkaraju A, Rodriguez-Boulan E. Itinerant exosomes: emerging roles in cell and tissue polarity. *Trends Cell Biol* 2008;18:199–209.
- Iero M, Valenti R, Huber V, Filipazzi P, Parmiani G, Fais S, et al. Tumour-released exosomes and their implications in cancer immunity. *Cell Death Differ* 2008;15:80–8.
- Taylor DD, Gercel-Taylor C. Tumour-derived exosomes and their role in cancer-associated T-cell signalling defects. *Br J Cancer* 2005;92:305–11.
- Liu C, Yu S, Zinn K, Wang J, Zhang L, Jia Y, et al. Murine mammary carcinoma exosomes promote tumor growth by suppression of NK cell function. *J Immunol* 2006;176:1375–85.
- Thery C, Ostrowski M, Segura E. Membrane vesicles as conveyors of immune responses. *Nat Rev Immunol* 2009;9:581–93.
- Hood JL, Pan H, Lanza GM, Wickline SA. Paracrine induction of endothelium by tumor exosomes. *Lab Invest* 2009;89:1317–28.
- Gesierich S, Berezovskiy I, Ryschich E, Zoller M. Systemic induction of the angiogenesis switch by the tetraspanin D6.1A/CO-029. *Cancer Res* 2006;66:7083–94.
- Nazarenko I, Rana S, Baumann A, McAlear J, Hellwig A, Trendelenburg M, et al. Cell surface tetraspanin Tspan8 contributes to molecular pathways of exosome-induced endothelial cell activation. *Cancer Res* 2010;70:1668–78.
- Sheldon H, Heikamp E, Turley H, Dragovic R, Thomas P, Oon CE, et al. New mechanism for Notch signaling to endothelium at a distance by Delta-like 4 incorporation into exosomes. *Blood* 2010;116:2385–94.
- Thery C, Clayton A, Amigorena S, Raposo G. Isolation and characterization of exosomes from cell culture supernatants and biological fluids. *Current Protocols in Cell Biology* 2006;Chapter 3: Unit3.22.
- Heijnen HF, Schiel AE, Fijnheer R, Geuze HJ, Sixma JJ. Activated platelets release two types of membrane vesicles: microvesicles by surface shedding and exosomes derived from exocytosis of multivesicular bodies and alpha-granules. *Blood* 1999;94:3791–9.
- Harrell MI, Iritani BM, Ruddell A. Lymph node mapping in the mouse. *J Immunol Methods* 2008;332:170–4.
- Mane VP, Heuer MA, Hillyer P, Navarero MB, Rabin RL. Systematic method for determining an ideal housekeeping gene for real-time PCR analysis. *J Biomol Tech* 2008;19:342–7.

Disclosure of Potential Conflicts of Interest

The authors have no competing financial interests to declare.

Authors' Contributions

J.L. Hood and S.A. Wickline devised experiments and wrote and edited the manuscript. J.L. Hood is the principle investigator of the exosome project and carried out and analyzed the experiments. S. San Roman developed procedures for the isolation, processing, and histologic analysis of lymph nodes. All authors read and approved the final version of the manuscript.

Acknowledgments

The authors thank Stacy J. Allen who provided expertise in animal care and Michael J. Scott who cultured cells, isolated exosomes, and assisted with injections.

Grant Support

Financial support and encouragement for this work was provided by The Role of Melanoma Exosomes in Angiogenesis (Elsa U. Pardee Foundation) and Induction of Angiogenic Nodal Turf by Melanoma Exosomes (Barnes-Jewish Hospital and Washington University in Saint Louis Siteman Cancer Center through the Research Development Award in Developmental Therapeutics) to J.L. Hood; and The Siteman Center of Cancer Nanotechnology Excellence at Washington University (NIH- U54 CA119342) and Methods in Molecular Imaging and Targeted Therapeutics (NIH- R01 HL073646) to S. San Roman and S.A. Wickline.

The costs of publication of this article were defrayed in part by the payment of page charges. This article must therefore be hereby marked *advertisement* in accordance with 18 U.S.C. Section 1734 solely to indicate this fact.

Received December 9, 2010; revised March 7, 2011; accepted March 27, 2011; published OnlineFirst April 8, 2011.

23. Valadi H, Ekstrom K, Bossios A, Sjostrand M, Lee JJ, Lotvall JO. Exosome-mediated transfer of mRNAs and microRNAs is a novel mechanism of genetic exchange between cells. *Nat Cell Biol* 2007;9:654-9.
24. Taylor DD, Gercel-Taylor C. MicroRNA signatures of tumor-derived exosomes as diagnostic biomarkers of ovarian cancer. *Gynecol Oncol* 2008;110:13-21.
25. Skog J, Wurdinger T, van Rijn S, Meijer DH, Gainche L, Sena-Esteves M, et al. Glioblastoma microvesicles transport RNA and proteins that promote tumour growth and provide diagnostic biomarkers. *Nat Cell Biol* 2008;10:1470-6.
26. Laulagnier K, Motta C, Hamdi S, Roy S, Fauvelle F, Pageaux JF, et al. Mast cell- and dendritic cell-derived exosomes display a specific lipid composition and an unusual membrane organization. *Biochem J* 2004;380:161-71.
27. Trajkovic K, Hsu C, Chiantia S, Rajendran L, Wenzel D, Wieland F, et al. Ceramide triggers budding of exosome vesicles into multivesicular endosomes. *Science* 2008;319:1244-7.
28. Parolini I, Federici C, Raggi C, Lugini L, Palleschi S, De Milito A, et al. Microenvironmental pH is a key factor for exosome traffic in tumor cells. *J Biol Chem* 2009;284:34211-22.
29. Goerdt S, Bhardwaj R, Sorg C. Inducible expression of MS-1 high-molecular-weight protein by endothelial cells of continuous origin and by dendritic cells/macrophages *in vivo* and *in vitro*. *Am J Pathol* 1993;142:1409-22.
30. Yang NY, Pasquale EB, Owen LB, Ethell IM. The EphB4 receptor-tyrosine kinase promotes the migration of melanoma cells through Rho-mediated actin cytoskeleton reorganization. *J Biol Chem* 2006;281:32574-86.
31. Yang NY, Lopez-Bergami P, Goydos JS, Yip D, Walker AM, Pasquale EB, et al. The EphB4 receptor promotes the growth of melanoma cells expressing the ephrin-B2 ligand. *Pigment Cell Melanoma Res* 2010;23:684-7.
32. Nip J, Shibata H, Loskutoff DJ, Cheresh DA, Brodt P. Human melanoma cells derived from lymphatic metastases use integrin alpha v beta 3 to adhere to lymph node vitronectin. *J Clin Invest* 1992;90:1406-13.
33. Montero L, Nagamine Y. Regulation by p38 mitogen-activated protein kinase of adenylate- and uridylylate-rich element-mediated urokinase-type plasminogen activator (uPA) messenger RNA stability and uPA-dependent *in vitro* cell invasion. *Cancer Res* 1999;59:5286-93.
34. Min HY, Doyle LV, Vitt CR, Zandonella CL, Stratton-Thomas JR, Shuman MA, et al. Urokinase receptor antagonists inhibit angiogenesis and primary tumor growth in syngeneic mice. *Cancer Res* 1996;56:2428-33.
35. Sund M, Kalluri R. Tumor stroma derived biomarkers in cancer. *Cancer Metastasis Rev* 2009;28:177-83.
36. Patarroyo M, Tryggvason K, Virtanen I. Laminin isoforms in tumor invasion, angiogenesis and metastasis. *Semin Cancer Biol* 2002;12:197-207.
37. Offermanns S, Mancino V, Revel JP, Simon MI. Vascular system defects and impaired cell chemokinesis as a result of Galpha13 deficiency. *Science* 1997;275:533-6.
38. Salven P, Lymboussaki A, Heikkila P, Jaaskela-Saari H, Enholm B, Aase K, et al. Vascular endothelial growth factors VEGF-B and VEGF-C are expressed in human tumors. *Am J Pathol* 1998;153:103-8.
39. Li X, Lee C, Tang Z, Zhang F, Arjunan P, Li Y, et al. VEGF-B: a survival, or an angiogenic factor? *Cell Adh Migr* 2009;3:322-7.
40. Mills CN, Joshi SS, Niles RM. Expression and function of hypoxia inducible factor-1 alpha in human melanoma under non-hypoxic conditions. *Mol Cancer* 2009;8:104.
41. Bosserhoff AK. Novel biomarkers in malignant melanoma. *Clin Chim Acta* 2006;367:28-35.
42. Giatromanolaki A, Sivridis E, Kouskourakis C, Gatter KC, Harris AL, Koukourakis MI. Hypoxia-inducible factors 1alpha and 2alpha are related to vascular endothelial growth factor expression and a poorer prognosis in nodular malignant melanomas of the skin. *Melanoma Res* 2003;13:493-501.
43. Isenber JS, Yu C, Roberts DD. Differential effects of ABT-510 and a CD63-binding peptide derived from the type 1 repeats of thrombospondin-1 on fatty acid uptake, nitric oxide signaling, and caspase activation in vascular cells. *Biochem Pharm* 2008;75:875-82.
44. Li B, Vincent A, Cates J, Brantley-Sieders DM, Polk DB, Young PP. Low levels of tumor necrosis factor alpha increase tumor growth by inducing an endothelial phenotype of monocytes recruited to the tumor site. *Cancer Res* 2009;69:338-48.
45. Valenti R, Huber V, Filipazzi P, Pilla L, Sovena G, Villa A, et al. Human tumor-released microvesicles promote the differentiation of myeloid cells with transforming growth factor-beta-mediated suppressive activity on T lymphocytes. *Cancer Res* 2006;66:9290-8.
46. Valenti R, Huber V, Iero M, Filipazzi P, Parmiani G, Rivoltini L. Tumor-released microvesicles as vehicles of immunosuppression. *Cancer Res* 2007;67:2912-5.
47. El-Hefnawy T, Raja S, Kelly L, Bigbee WL, Kirkwood JM, Luketich JD, et al. Characterization of amplifiable, circulating RNA in plasma and its potential as a tool for cancer diagnostics. *Clin Chem* 2004;50:564-73.